CO in Protostars

Herschel-SPIRE Spectroscopy of Embedded Protostars (COPS-SPIRE)

Yao-Lun Yang
The University of Texas at Austin
Jul. 4 2017, 2017 APRIM

CO in Protostars

Herschel-SPIRE Spectroscopy of Embedded Protostars (COPS-SPIRE)

Collaborators:
Joel Green, Neal Evans, Jeong-Eun Lee, Jes Jørgensen,
Joseph Mottram, Lars Kristensen, Edwin Bergin, Odysseas Dionatos,
Jeroen Bouwman, Gregory Herczeg, Ewine van Dishoeck, Agata Karska,
Tim van Kempen, Rebecca Larson, and Umut Yıldız

Active star formation within embedded protostars

- Embedded protostars are at the earliest stage of star formation.
- The envelope provides abundant dust and gas for the growth of protostar. The mass accretion/ejection occurred at the embedded phase determines the conditions for disk evolution and planet formation.
  (e.g. Jorgensen+2009, Kristensen+2012, Yen+2015)
- Active outflows and jets, resulting from the mass infall/accretion, also feedbacks to the envelope.
  (e.g. Offner+2014, Nisini+2015, Yıldız+2015)

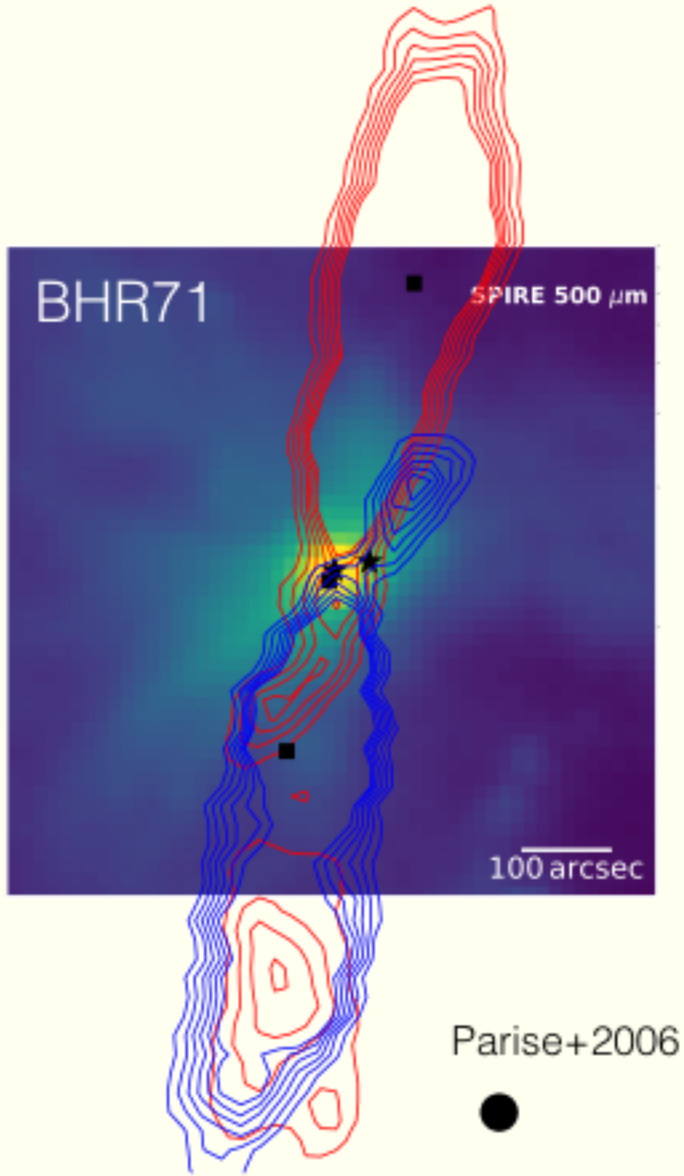

Sampling a wide range of source properties

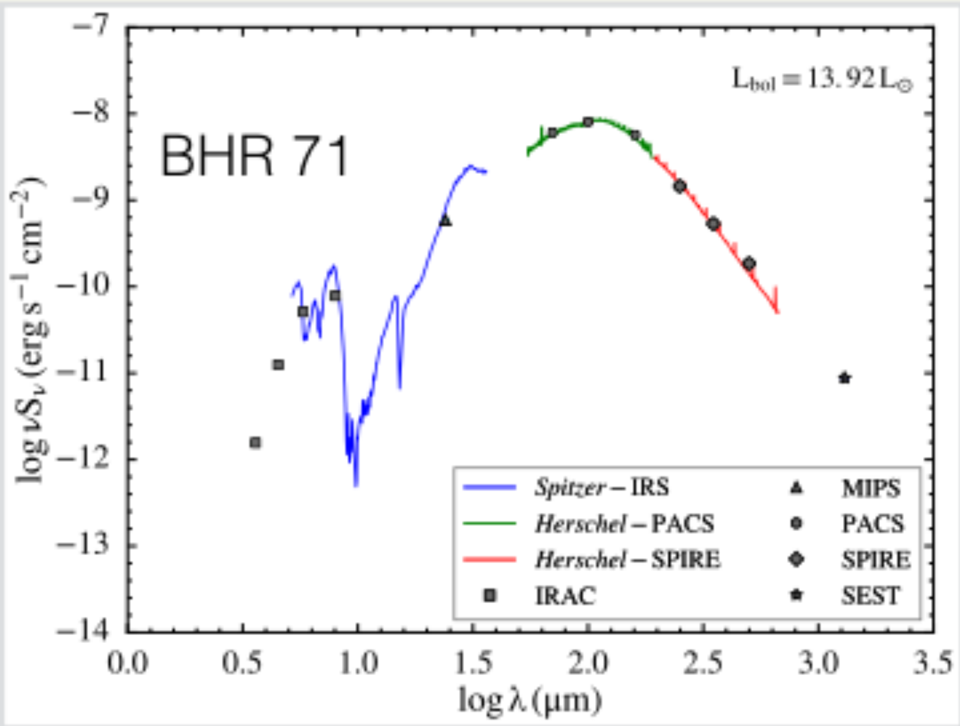

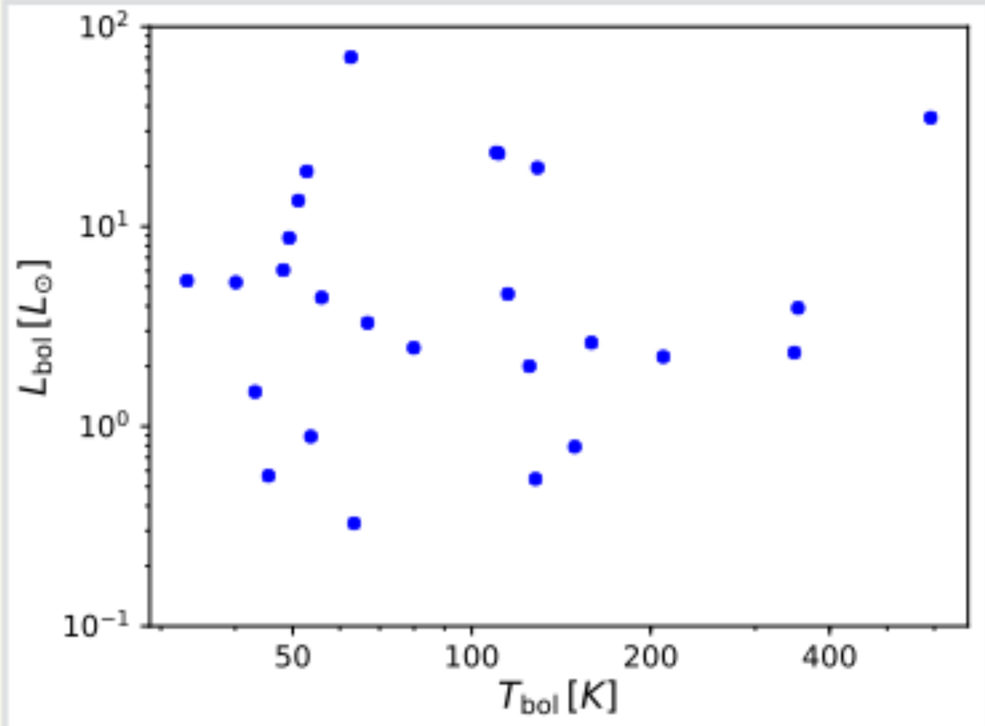

Yang+2017

What physical processes drive the early stage of star formation?

What physical processes drive the early stage of star formation?

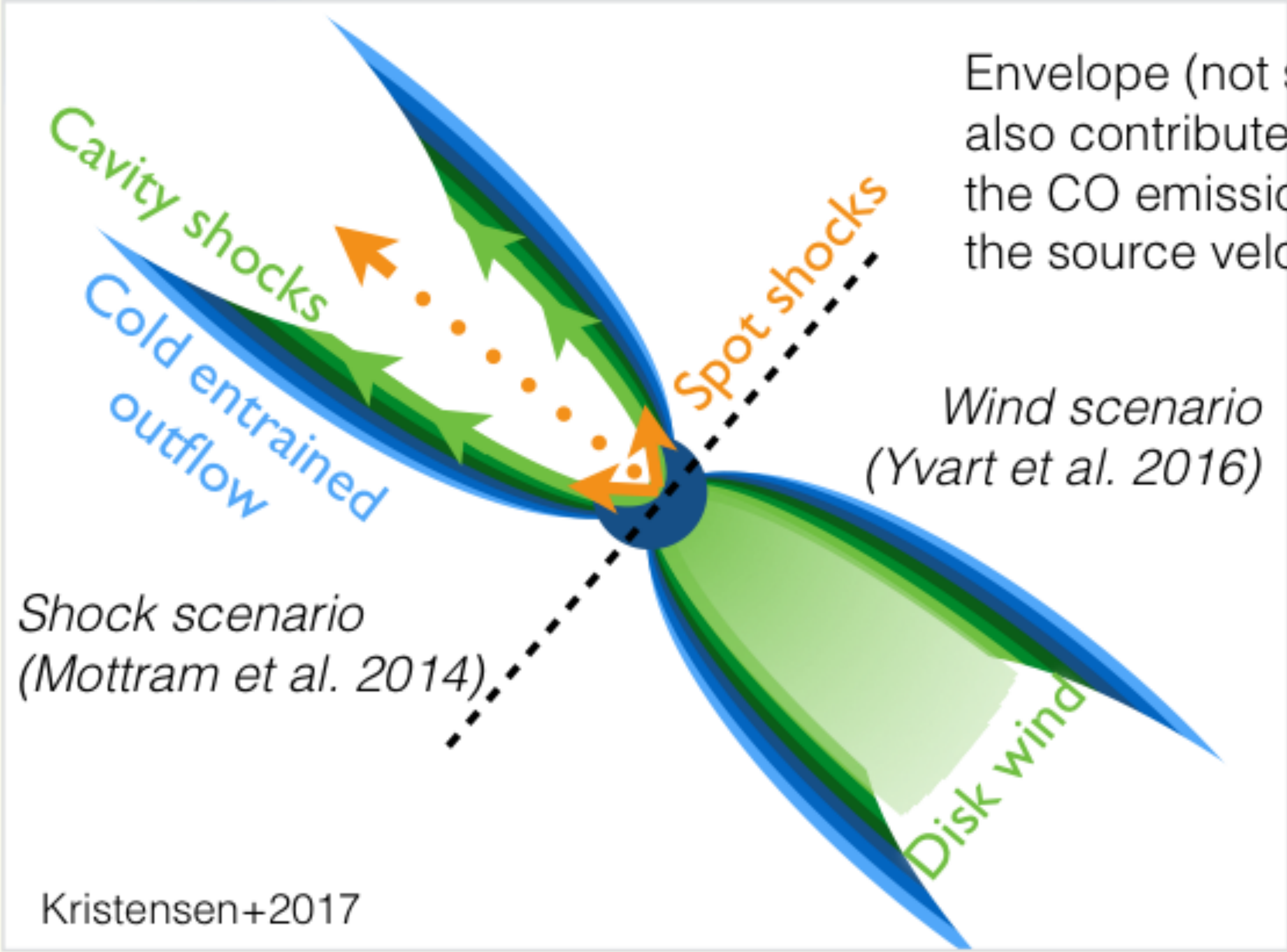

A single CO emission line exhibits multiple velocity

components

CO $J = 16 \rightarrow 15$ velocity-resolved spectra

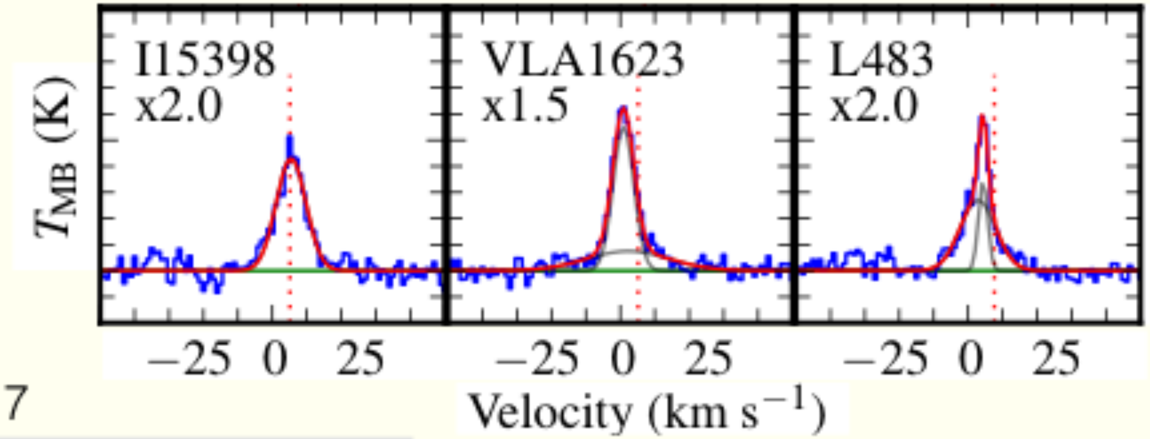

Kristensen+2017

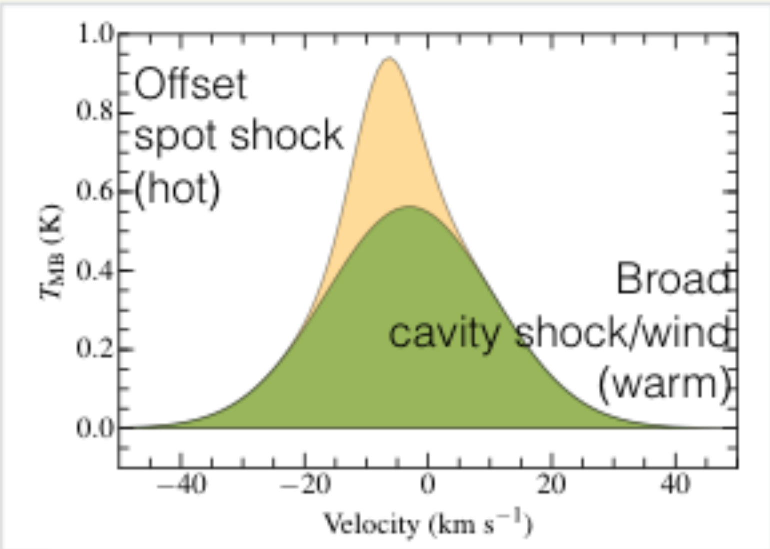

For CO $J = 16 \rightarrow 15$:

20% spot shock

80% cavity shock/wind

Correlations of CO Emission Lines:

From $J = 4 \rightarrow 3$ to $J = 36 \rightarrow 35$

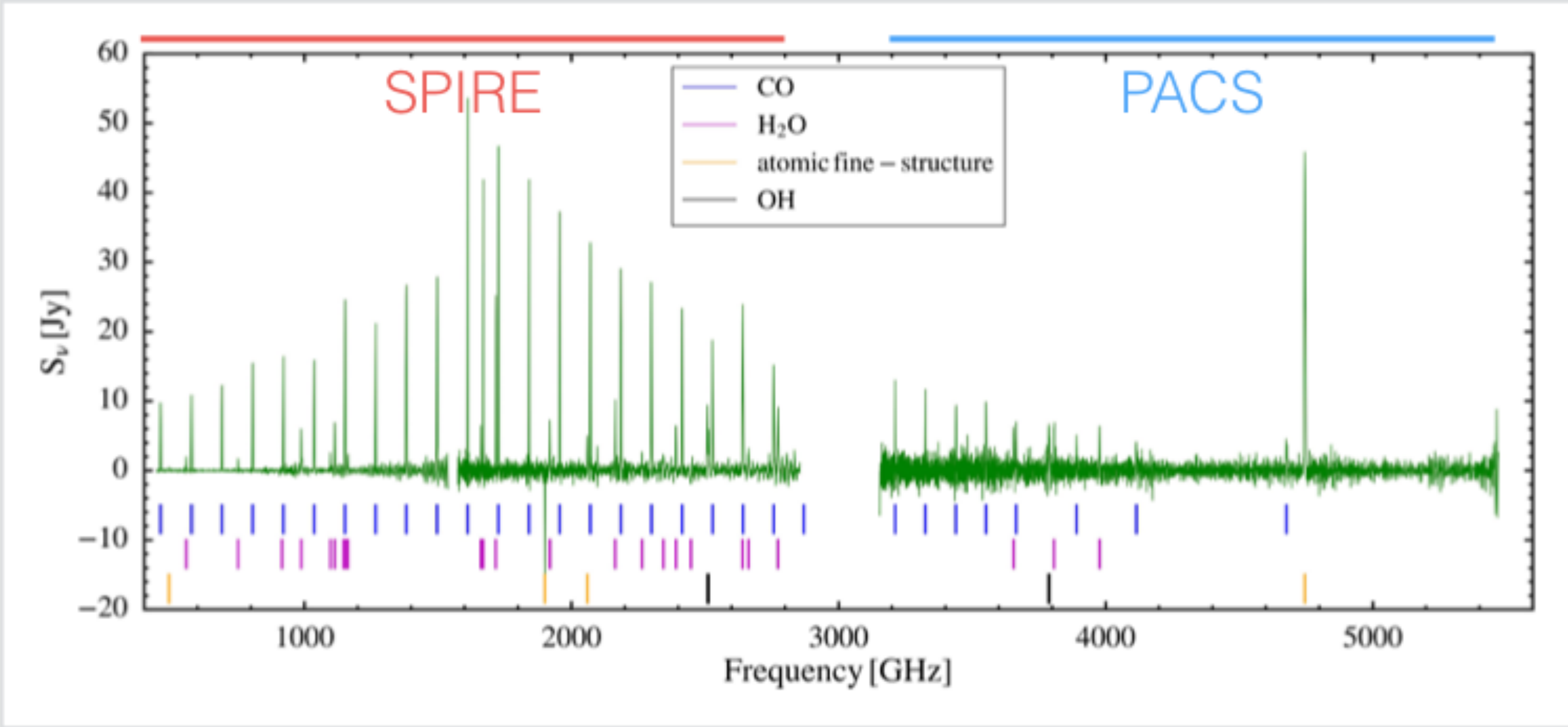

Correlations of CO Emission Lines:

From $J = 4 \rightarrow 3$ to $J = 36 \rightarrow 35$

From J = 4→3 to J = 36→35

Spearman's ρ: the goodness of the relation can be described by a monotonic function, including the upper limits.

$\rho = 0.794, 4.4\sigma$

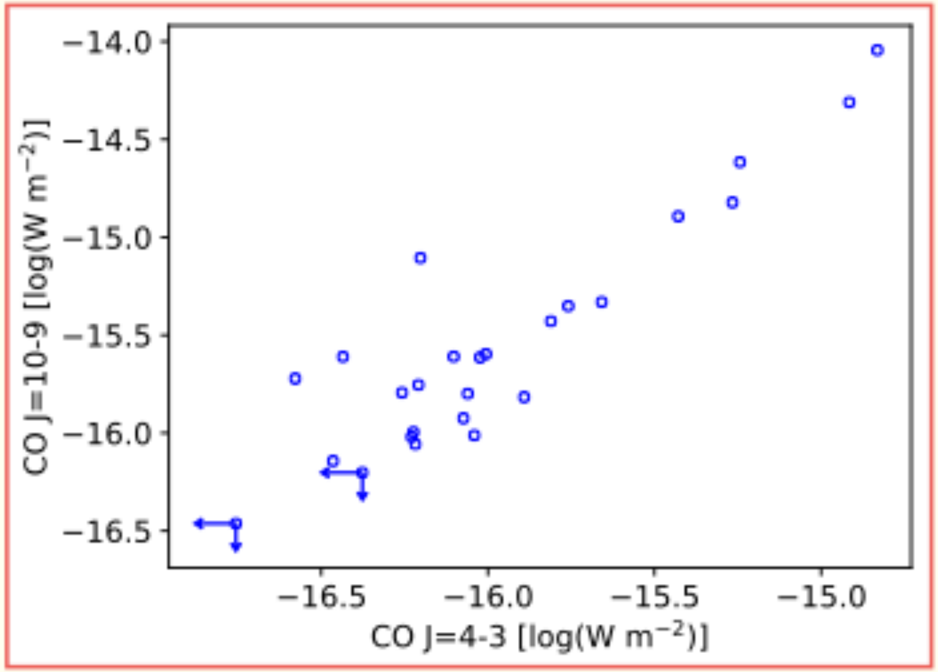

$\rho = 0.509, 2.7\sigma$

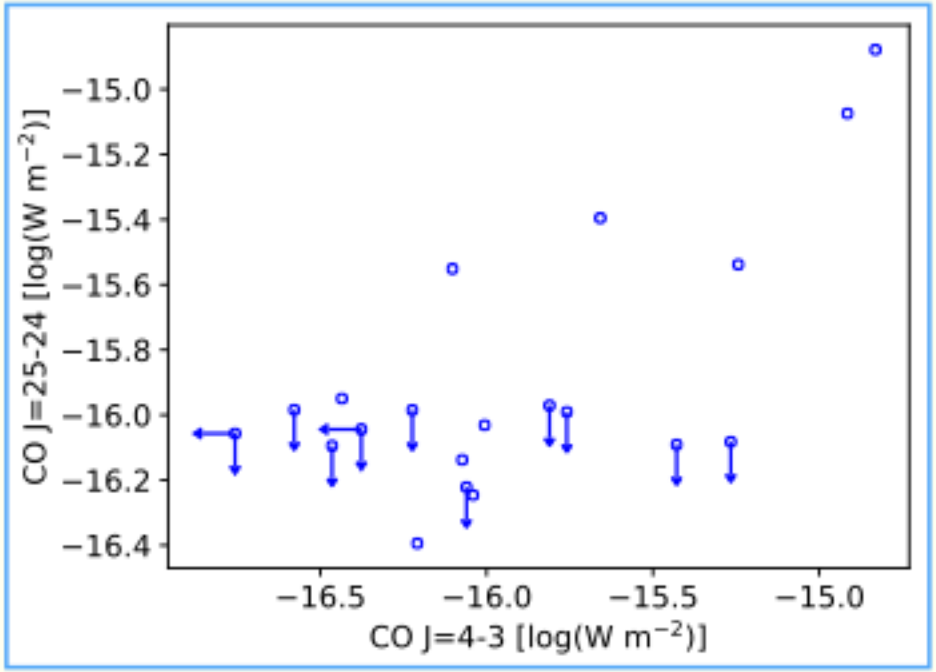

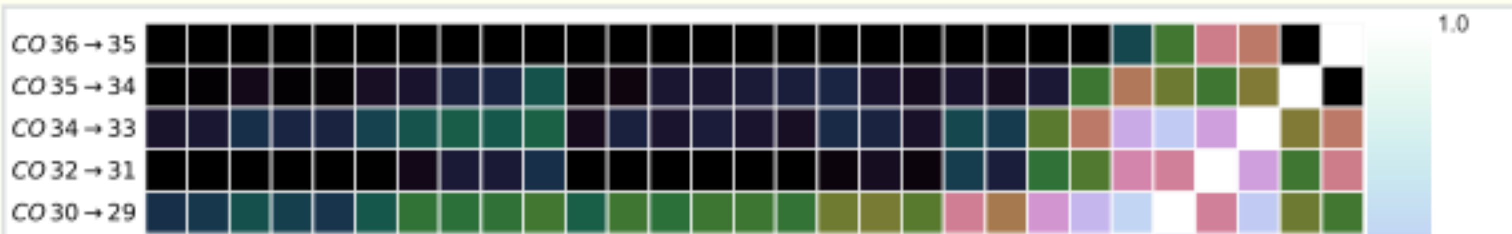

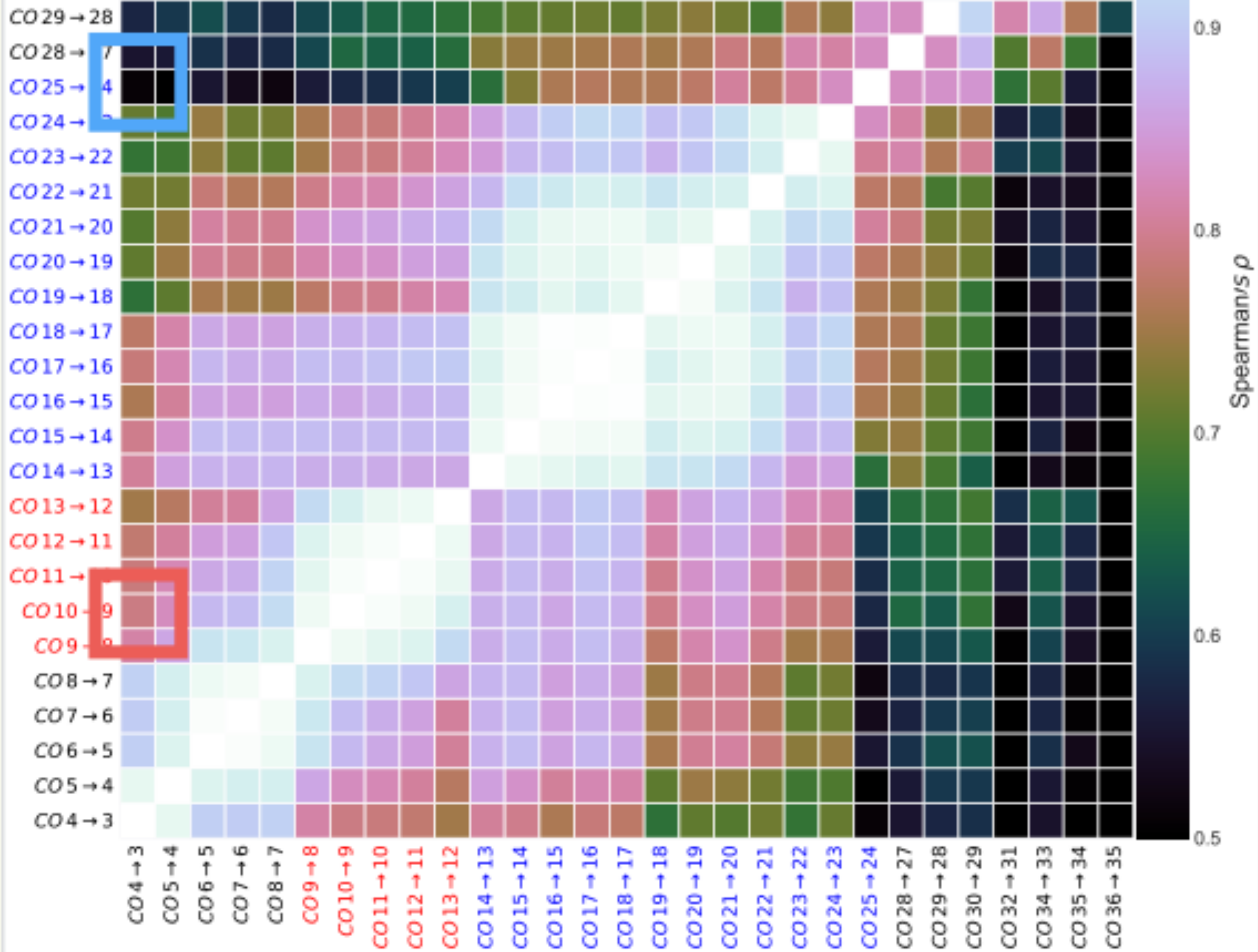

How to interpret the CO emission?

Velocity-resolved spectra -

Multiple origins contribute to a single line.

Smooth variation of correlation strength -

Each excitation process contributes to the CO emission with a wide range of *J*-levels.

We need both information to fully model the CO emission; furthermore, constrain the underlying physical processes.

Bipolar morphology of CO emission

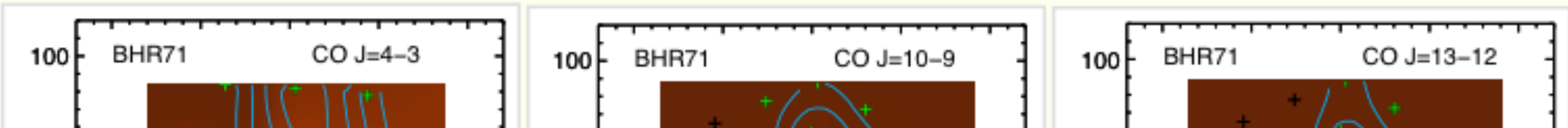

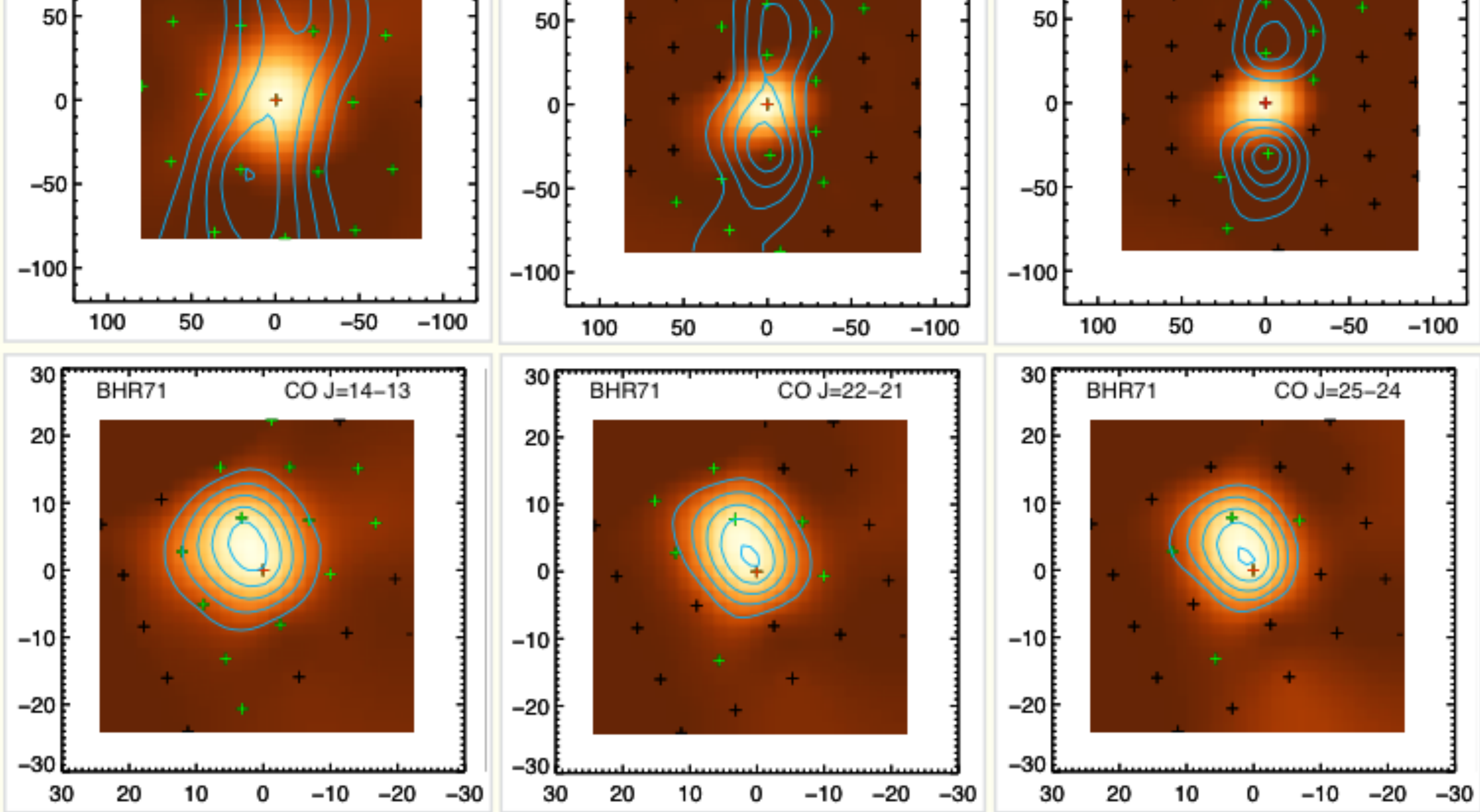

How to systematically study the morphology of CO emission?

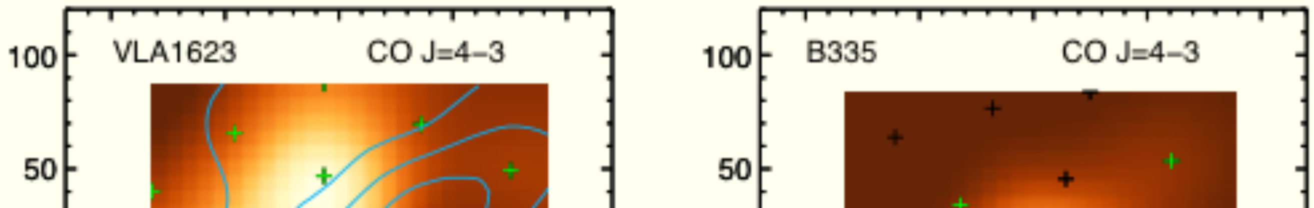

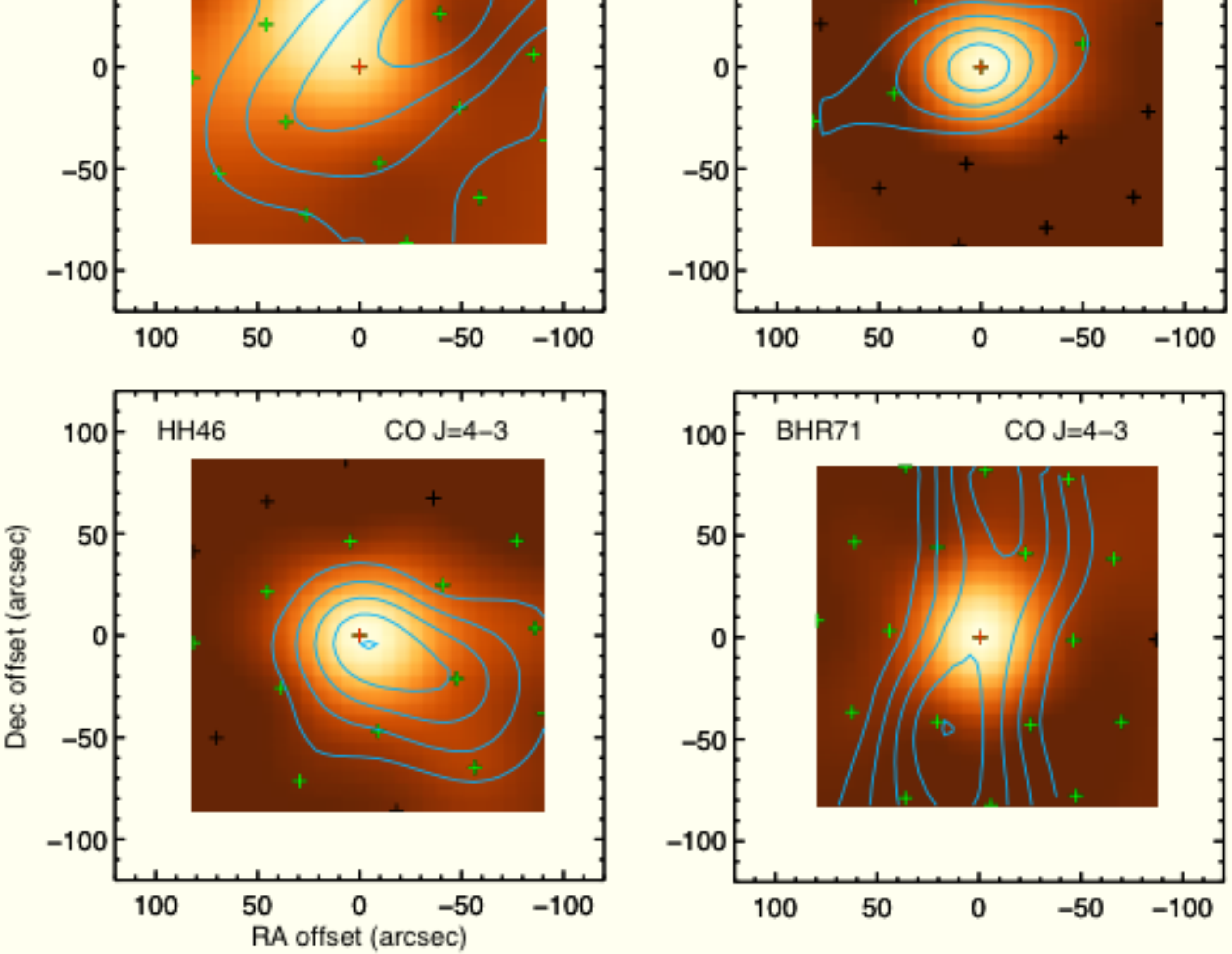

Yao-Lun Yang | UT-Austin

Spatial Extent of CO Emission

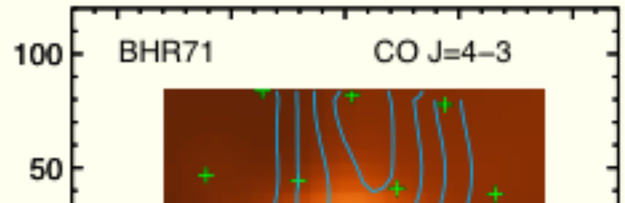

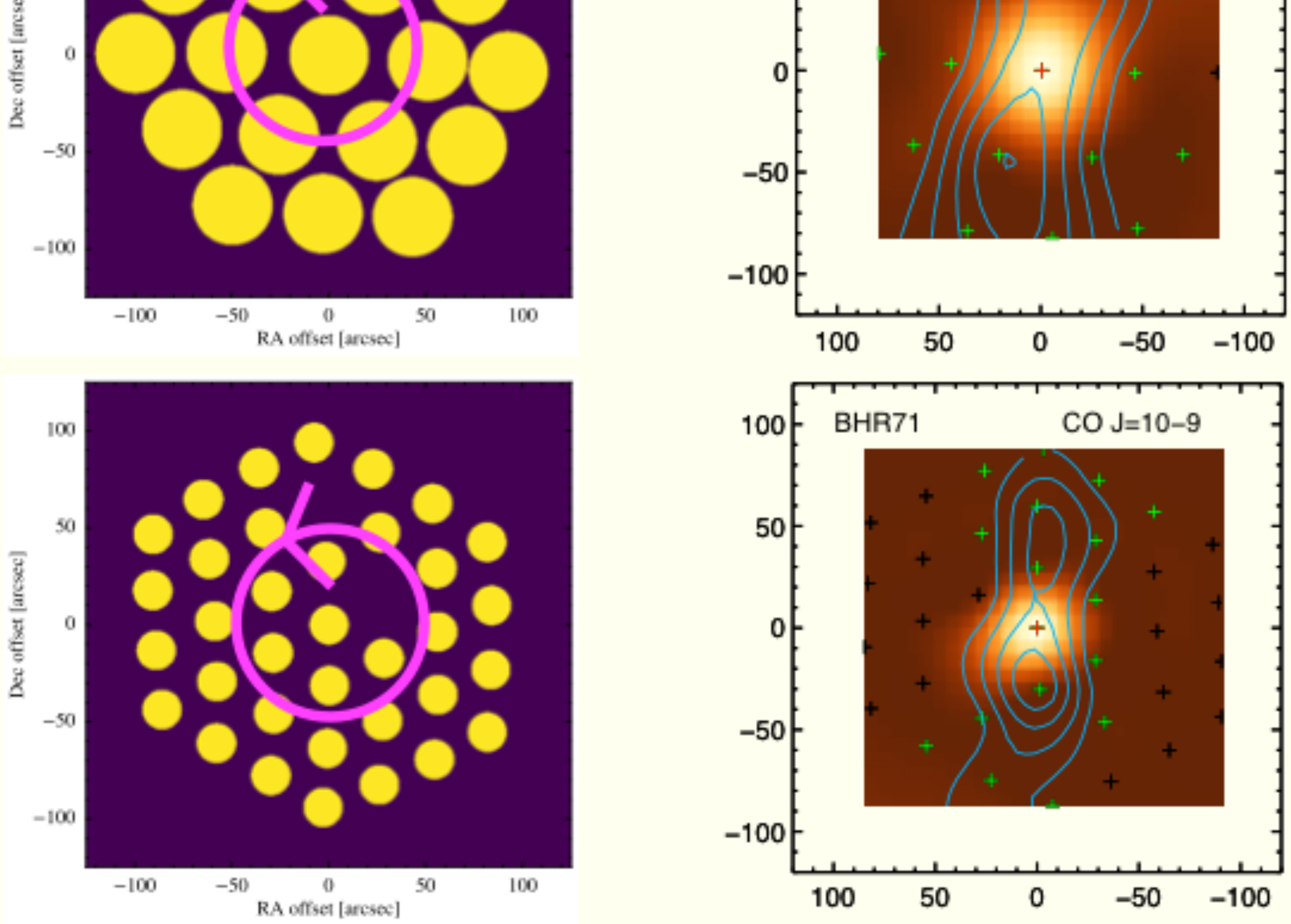

Spatial Extent of CO Emission

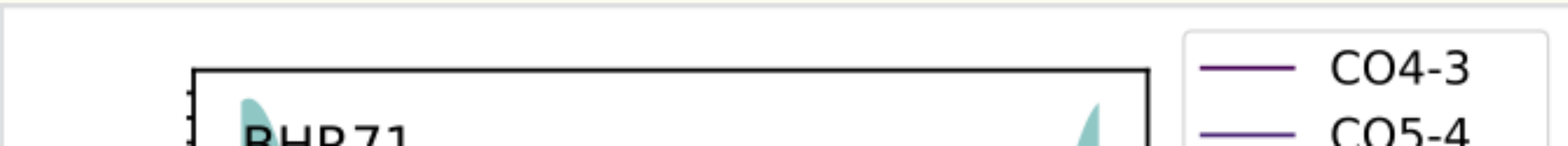

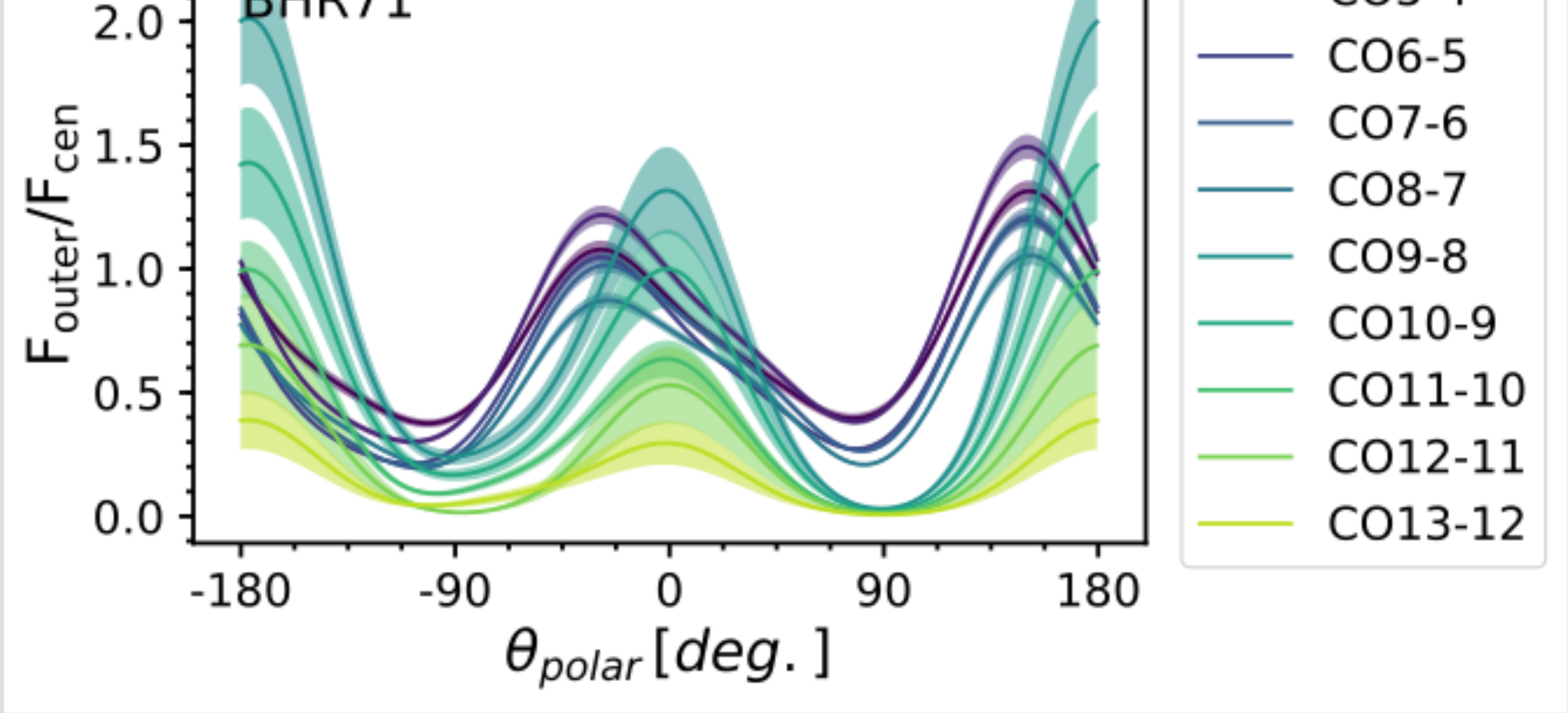
BHR71
CO6-5
CO7-6
CO8-7
CO9-8
CO10-9
CO11-10
CO12-11
CO13-12
F_{outer}/F_{cen}
$\theta_{polar}\,[deg.]$
-180
-90
0
90
180
0.0
0.5
1.0
1.5
2.0

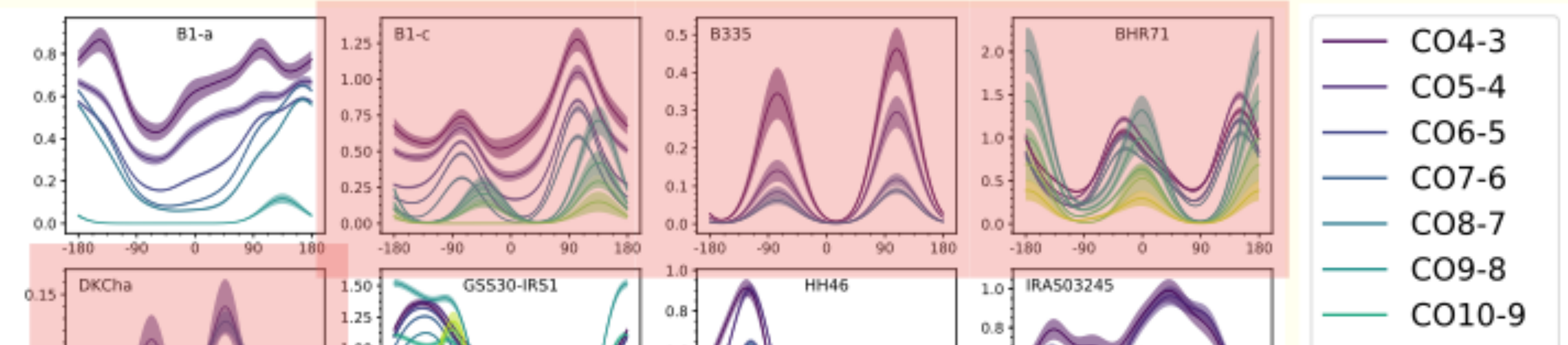
B1-a
B1-c
B335
BHR71
DKCha
GSS30-IRS1
HH46
IRAS03245
CO4-3
CO5-4
CO6-5
CO7-6
CO8-7
CO9-8
CO10-9

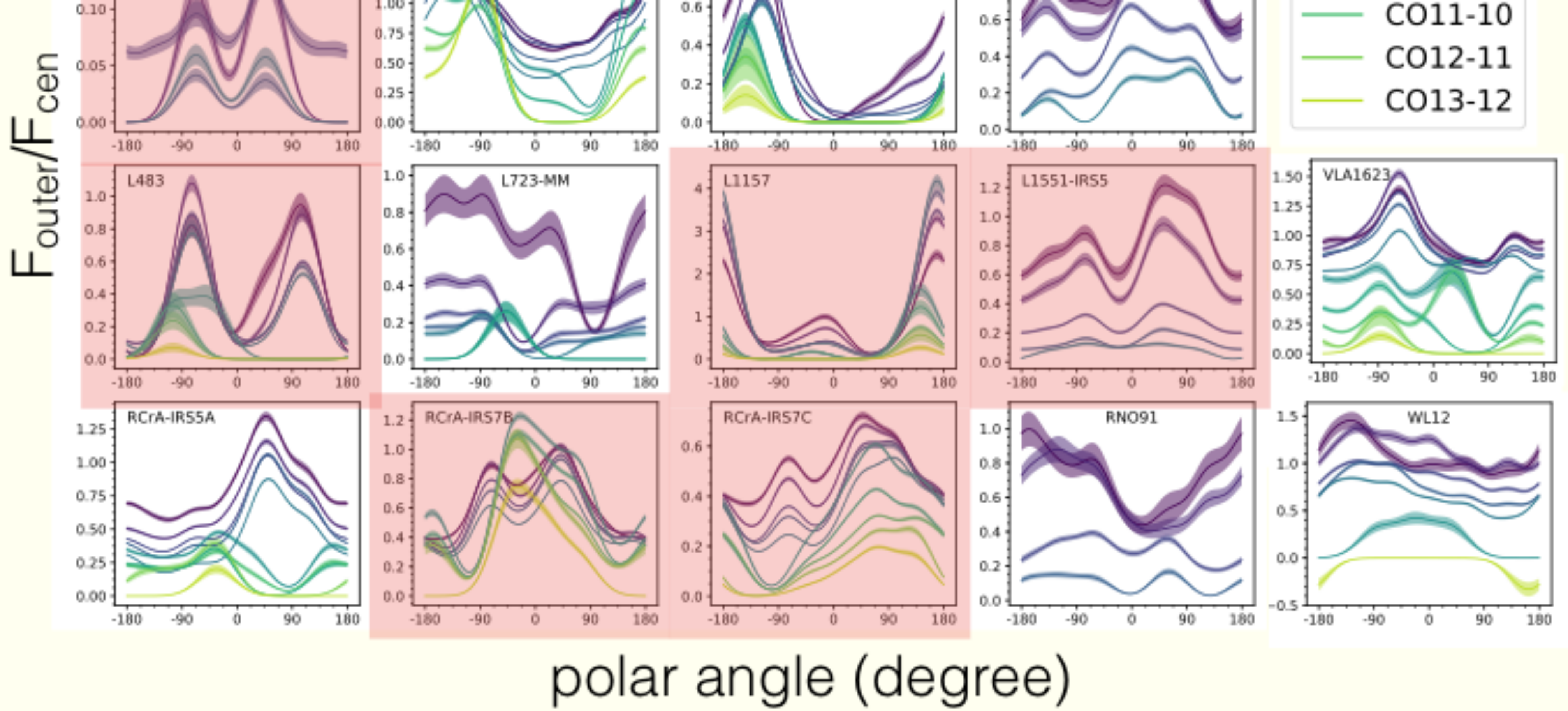

Yao-Lun Yang | UT-Austin

The variation of bipolar feature as a function of *J*-level

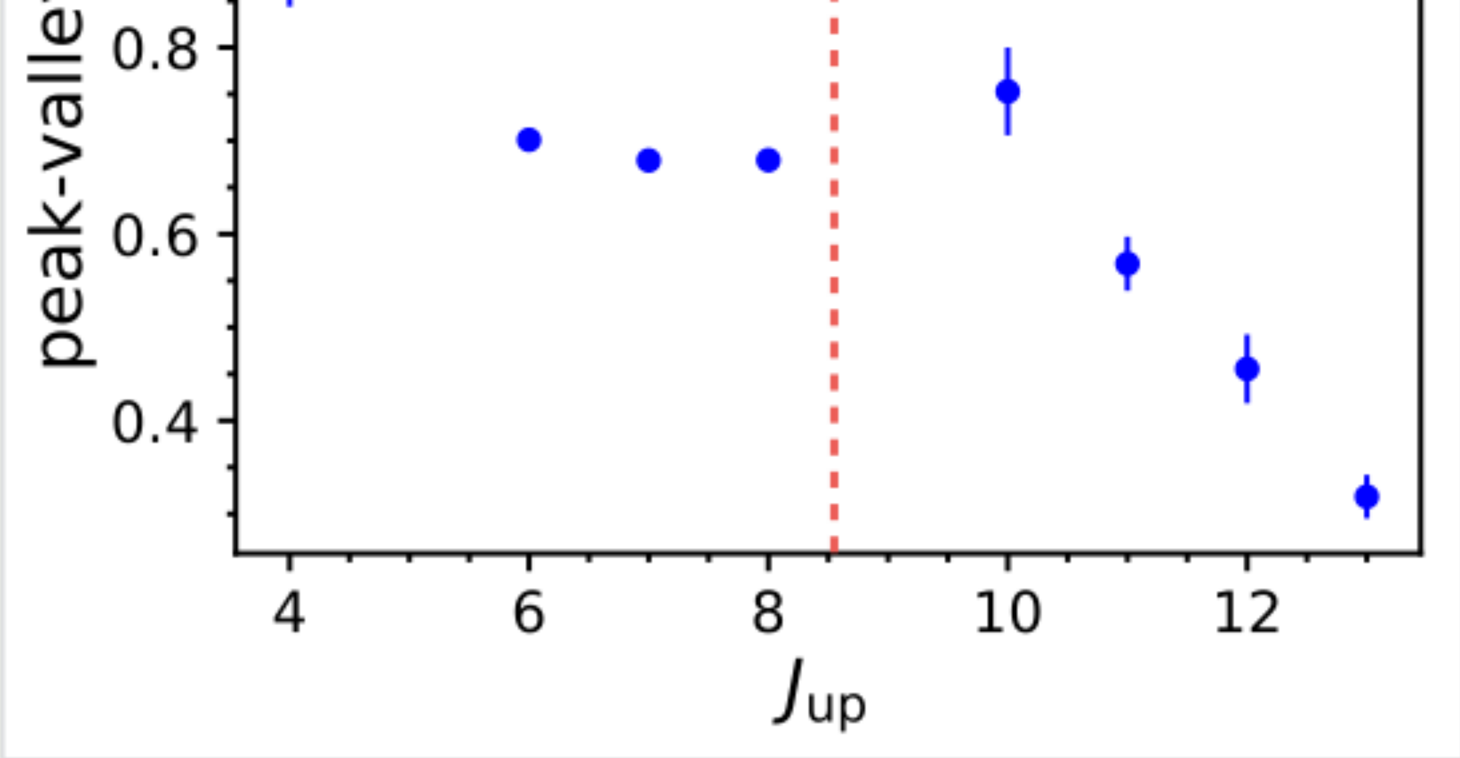

Summary

- The correlations of CO suffer from the instrumental systematic biases. Within the coverage of each module, the correlation shows a smooth variation without sharp edges.
- The velocity-resolved spectra of CO show multiple velocity

components (Kristensen+2017). The smooth distribution of the correlation strength indicates that each excitation mechanism contributes to a wide range of CO rotational lines.

- We develop a new method to visualize the morphology of the CO emission from *Herschel* data by comparing the flux ratio to the central spaxel and smoothing the profile as a function of polar angle.
- Bipolar features are found in 50% of the sources at low-*J* CO lines, which may decrease as the *J*-level increases.